

# Inhibition of ABCG2 prevents phototoxicity in a mouse model of erythropoietic protoporphyria

Received: 8 February 2024

Accepted: 21 November 2024

Published online: 04 December 2024

 Check for updates

Junjie Zhu<sup>1</sup>, Fu-Ying Qin<sup>1</sup>, Saifei Lei<sup>1</sup>, Ruizhi Gu<sup>1</sup>, Qian Qi<sup>1</sup>, Jie Lu<sup>1</sup>, Karl E. Anderson<sup>2</sup>, Peter Wipf<sup>3</sup> & Xiaochao Ma<sup>1</sup>✉

Erythropoietic protoporphyria (EPP) is a genetic disease characterized by protoporphyrin IX-mediated painful phototoxicity. Currently, options for the management of EPP-associated phototoxicity are limited and no oral medication is available. Here, we investigated a novel therapy against EPP-associated phototoxicity by targeting the ATP-binding cassette subfamily G member 2 (ABCG2), the efflux transporter of protoporphyrin IX. Oral ABCG2 inhibitors were developed, and they successfully prevented EPP-associated phototoxicity in a genetically engineered EPP mouse model. Mechanistically, ABCG2 inhibitors suppress protoporphyrin IX release from erythroid cells and reduce the systemic exposure to protoporphyrin IX in EPP. In summary, our work establishes a novel strategy for EPP therapy by targeting ABCG2 and provides oral ABCG2 inhibitors that can effectively prevent protoporphyrin IX-mediated phototoxicity in mice.

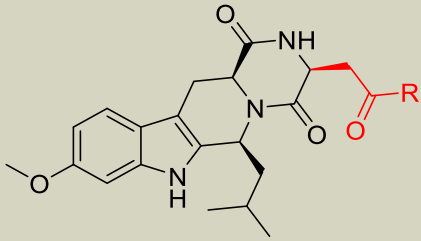
Erythropoietic protoporphyria (EPP) is an inherited disease caused by loss-of-function mutations of ferrochelatase (FECH)<sup>1,2</sup>, the final enzyme in the heme biosynthesis pathway that converts protoporphyrin IX (PPIX) to heme. A deficiency of FECH disrupts PPIX metabolism and leads to PPIX accumulation in the body<sup>1,3</sup>. PPIX is photoactive because it contains the electron-rich tetrapyrrole moiety<sup>4,5</sup>. Once PPIX is excited by sunlight, it produces reactive oxygen species (ROS), subsequently resulting in cellular damages in the skin<sup>4,6</sup>. Due to phototoxicity-induced pain, EPP patients have to wear protective clothing and limit outdoor activities, which markedly impair their quality of life<sup>7,8</sup>. Children with EPP struggle with the disease and find it difficult to navigate school life<sup>7</sup>.

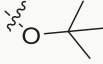
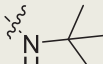
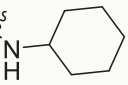
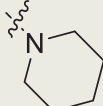
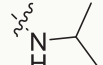
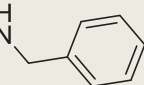
Limited options are currently available for the management of EPP-associated phototoxicity. Afamelanotide is a synthetic analog of  $\alpha$ -melanocyte-stimulating hormone, which increases skin pigmentation, decreases the penetration depth of light into the skin, and thus helps to prevent PPIX-mediated phototoxicity<sup>9</sup>. Afamelanotide is approved by the FDA for the prevention of EPP-associated phototoxicity in adults but not children<sup>10</sup>, even though EPP is the most common porphyria in

children<sup>8,11</sup>. In addition, afamelanotide is provided as a subcutaneous implant<sup>10</sup>, which is inconvenient for patients. Multiple antioxidants have also been considered for alleviating EPP-associated phototoxicity<sup>12–15</sup>, but their effectiveness has not been fully confirmed in clinical studies or by patient experience<sup>12,13,16</sup>. Therefore, novel therapeutic approaches are needed for the management of PPIX-mediated phototoxicity in EPP.

Under EPP condition, PPIX is primarily produced in bone marrow and accumulated in erythroid cells<sup>1,3</sup>. The ATP-binding cassette subfamily G member 2 (ABCG2) pumps PPIX out of erythroid cells into the plasma<sup>17,18</sup>, leading to the exposure of PPIX to the skin and resulting in phototoxicity when PPIX is excited by sunlight. Our recent work established an important role of ABCG2 in PPIX-mediated phototoxicity by finding that phototoxicity was abolished in an EPP mouse model deficient in ABCG2<sup>19</sup>. These data suggest that ABCG2 is a promising target for preventing phototoxicity in EPP. The present work investigated the therapeutic potential of ABCG2 inhibitors against EPP-associated phototoxicity. Oral ABCG2 inhibitors were developed and their efficacy was evaluated in an EPP mouse model caused by a loss-of-function mutation of FECH (Fech-mut)<sup>20,21</sup>. Our results revealed that

<sup>1</sup>Center for Pharmacogenetics, Department of Pharmaceutical Sciences, School of Pharmacy, University of Pittsburgh, Pittsburgh, PA, USA. <sup>2</sup>Porphyria Laboratory & Center, Department of Internal Medicine, University of Texas Medical Branch, Galveston, TX, USA. <sup>3</sup>Department of Chemistry, University of Pittsburgh, Pittsburgh, PA, USA. ✉e-mail: [mxiaocha@pitt.edu](mailto:mxiaocha@pitt.edu)

**Table 1 | Characterization of newly developed Ko143 analogs**


Cpd	R	IC <sub>50</sub> (μM)	CC <sub>50</sub> (μM)	Stability in HLM (% remaining)	
				30 min	60 min
Ko143		0.18 ± 0.08	22.3 ± 0.6	6 ± 0.8	2 ± 1
K16	-OBzl	0.12 ± 0.01	49.6 ± 2.8	22 ± 4	9 ± 2
K17	-OH	15% @ 1 μM	N.D.	N.D.	N.D.
K3		0.18 ± 0.12	58.9 ± 5.3	74 ± 25	60 ± 3
K23		0.13 ± 0.07	46.6 ± 0.9	45 ± 2	26 ± 2
K25		3.14 ± 1.42	26.5 ± 2.5	N.D.	N.D.
K31		0.27 ± 0.04	> 100	65 ± 3	49 ± 9
K33		0.25 ± 0.06	31.1 ± 3.7	37 ± 3	18 ± 1

All data are expressed as mean ± SD ( $n \geq 3$ ). Source data are provided as a Source Data file. IC<sub>50</sub> half-maximal inhibitory concentration on ABCG2, CC<sub>50</sub> half-cytotoxic concentration, HLM human liver microsomes, N.D. not determined.

oral ABCG2 inhibitors can effectively prevent phototoxicity in EPP by modulating PPIX distribution.

## Results

### Development of oral ABCG2 inhibitors

We first tested the effect of Ko143, a classic ABCG2 inhibitor<sup>22</sup>, on PPIX-mediated phototoxicity in Fech-mut mice. These mice were pretreated orally with Ko143 followed by exposure to light (395–410 nm, the range of maximum absorption by PPIX) (Supplementary Fig. 1a). However, Ko143 failed to protect against PPIX-mediated phototoxicity because of its poor metabolic stability (Supplementary Fig. 1b, c). We next conducted metabolism-guided drug design to develop novel Ko143 analogs with better metabolic stability (Supplementary Fig. 2 and Table 1). K31 is a chain-truncated, isopropyl-substituted amide analog of Ko143 (Fig. 1a). K31 showed a similar ABCG2 inhibitory activity as Ko143 (Fig. 1b), but its metabolic stability was significantly improved in the incubation with human liver microsomes (Fig. 1c). In addition, studies in mice showed outstanding pharmacokinetic profiles of K31 after oral treatment (Fig. 1d). Furthermore, K31 is less cytotoxic when compared to other Ko143 analogs (Table 1). Moreover, the unbound fraction of K31 in mouse serum is 5.85%, and it has no inhibitory effect on ABCB1, also known as multidrug resistance protein 1 or P-glycoprotein 1 (Supplementary Fig. 3). These data suggest that K31 is an ideal candidate for evaluating the efficacy of ABCG2 inhibitors in preventing EPP-associated phototoxicity.

### Efficacy of oral ABCG2 inhibitors against EPP-associated phototoxicity

Using the same protocol as for Ko143 (Supplementary Fig. 1a), Fech-mut mice were pretreated orally with K31 followed by light exposure. Light-triggered phototoxicity was significantly decreased in the K31 groups (30 and 100 mg/kg) as shown by the gross appearance of the skin of Fech-mut mice in both sexes (Fig. 1e, f, Supplementary Fig. 4). Histological analysis revealed that the epidermis of skin was missing and subepidermal collagen was damaged in the control group of Fech-mut mice after light exposure, but these changes were prevented in the groups with K31 treatment (Fig. 2a, b, Supplementary Fig. 4). In addition, pretreatment with K31 attenuated oxidative stress and inflammation in the skin of Fech-mut mice exposed to light (Fig. 2c–e).

We noted the differences of histological findings in the skin between EPP mouse models and EPP patients, which can be explained by the followings: (1) the EPP mice received a high amount of irradiation without protection, whereas EPP patients usually avoid light with self-protection; and (2) the histological changes in the skin of EPP patients are built up for many years because of the repeated injury and repair, leading to the thickness of vessel walls (Timonen et al., 2000); but the current study on EPP-related phototoxicity in mice only lasted for several days. To further verify the efficacy of K31, a withdrawal test was conducted in Fech-mut mice. The recurrence of light-triggered phototoxicity was observed in the skin of Fech-mut mice from the second day of K31 withdrawal (Fig. 3, Supplementary Fig. 5), indicating the ABCG2 inhibitor-dependent effect against EPP-associated phototoxicity. Moreover, throughout multiple years of investigations in this project, we have been using both male and female mice and no significant sex difference was observed for the efficacy of ABCG2 inhibitors in preventing EPP-related phototoxicity.

### Mechanisms for the prevention of EPP-associated phototoxicity by ABCG2 inhibitors

After K31 treatment in Fech-mut mice, we observed a significant decrease of PPIX in serum (Fig. 4a). These results were consistent with the data from Fech-mut mice deficient in ABCG2 (Fech-mut/Abcg2-null mice), which showed a lower level of serum PPIX than in Fech-mut mice (Fig. 4b). The levels of PPIX in serum are determined by ABCG2 in erythroid cells<sup>17–19</sup>. The expression of ABCG2 in red blood cells (RBCs) was detected in Fech-mut mice but was absent in Fech-mut/Abcg2-null mice (Fig. 4c), which contributes to a significantly higher level of PPIX in the RBCs of Fech-mut/Abcg2-null mice than that in Fech-mut mice (Supplementary Fig. 6). The role of ABCG2 in PPIX efflux from RBCs was further investigated using genetic and pharmacologic approaches. As expected, the release of PPIX from the RBCs of Fech-mut/Abcg2-null mice was significantly lower than that in Fech-mut mice (Fig. 4d). Likewise, inhibition of ABCG2 by K31 also markedly decreased PPIX release from the RBCs of Fech-mut mice (Fig. 4e). These data suggest that suppression of ABCG2 blocks PPIX efflux from erythroid cells and decreases PPIX levels in plasma, consequently decreasing the systemic distribution of PPIX, reducing its exposure to the skin, and preventing phototoxicity in EPP (Fig. 4f).

### Safety of ABCG2 inhibitors for EPP therapy

We next evaluated the safety profile of K31 with a focus on its potential adverse effects on bone marrow, liver, and kidney, where ABCG2 is also expressed<sup>17,18,23</sup>. Biochemical analysis revealed that 5 days of treatment with K31 had no significant impact on the mean corpuscular hemoglobin and total hemoglobin in the blood of Fech-mut mice (Supplementary Fig. 7a, b). In addition, short-term treatment with K31 did not alter PPIX levels in the liver of Fech-mut mice (Supplementary Fig. 7c) and did not potentiate liver damage in Fech-mut mice, as indicated by the liver injury marker alanine aminotransferase (Supplementary Fig. 7d). Furthermore, short-term treatment with K31 did not cause morphological changes in the liver and kidney of Fech-mut mice

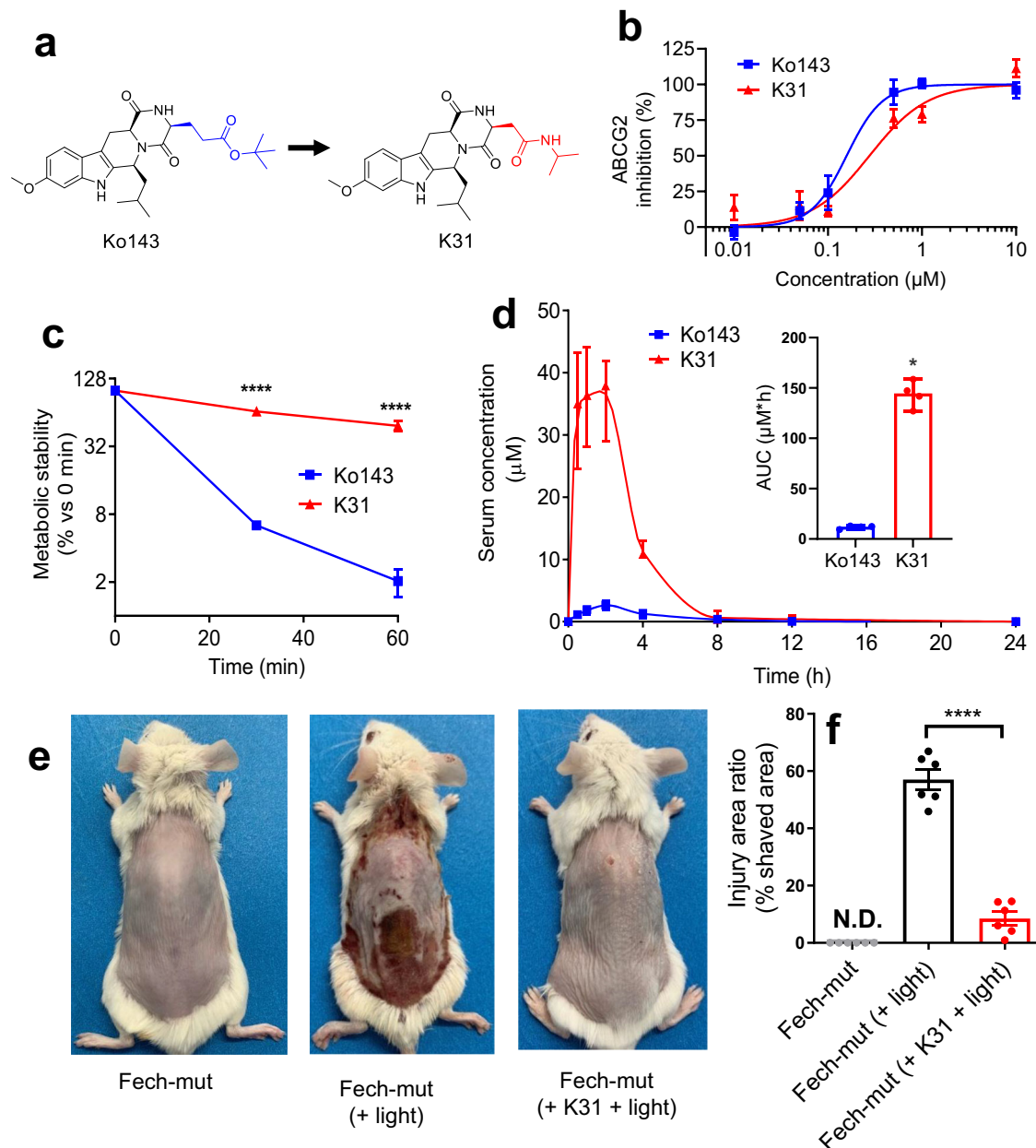


**Fig. 1 | The oral ABCG2 inhibitor K31 prevents phototoxicity in an EPP mouse model.** **a** The development of K31 through the structural modification of Ko143. **b** The inhibitory activity of K31 and Ko143 on ABCG2 ( $n = 4$  for each concentration). Data are expressed as mean  $\pm$  SEM. **c** Metabolic stability of Ko143 and K31 in incubations ( $n = 3$  for each time point) with human liver microsomes. Data are expressed as mean  $\pm$  SEM. \*\*\*\* $P < 0.0001$ , two-way ANOVA with Šidák's multiple comparisons test. **d** Pharmacokinetics of Ko143 and K31 in WT mice. Blood samples ( $n = 4$  for each time point) were collected from the mice treated with Ko143 or K31 (100 mg/kg, po). Ko143 and K31 in sera were analyzed by UPLC-QTOFMS. The inset

panel shows the areas under the curve (AUC) of Ko143 and K31. Data are expressed as median with range. \* $P = 0.0286$ , two-tailed Mann-Whitney test. **e, f** The effects of K31 on phototoxicity in Fech-mut mice (male). The back skin of Fech-mut mice was shaved, and they were then treated with K31 (100 mg/kg, po, once daily for 5 days). Forty min after K31 treatment, these mice were exposed to light for 20 min. **e** Gross appearance of the skin in Fech-mut mice pretreated with K31. **f** The ratio of injured areas vs shaved areas of skin. Data are expressed as mean  $\pm$  SEM ( $n = 6$  mice). \*\*\*\* $P < 0.0001$ , one-way ANOVA with Dunnett's multiple comparisons test. N.D. not detected. Source data are provided as a Source Data file.

(Supplementary Fig. 7e, f). Moreover, our sub-chronic study (23 days) in WT mice showed that treatment with K31 did not alter growth, the ratios of organ (liver, kidney, and spleen) to body weight, and the biomarkers of liver toxicity (Supplementary Figs. 8 and 9).

## Discussion

Using the newly developed ABCG2 inhibitors together with genetically engineered EPP mouse models, our work demonstrated that pharmacological inhibition of ABCG2 can effectively prevent PPIX-mediated phototoxicity in EPP. This ABCG2-inhibiting approach is

mechanistically different from the currently available methods used for preventing EPP-associated phototoxicity, such as drugs that increase skin pigmentation. In addition, our ABCG2-inhibiting approach will be convenient for clinical practice because ABCG2 inhibitors can be administered orally.

Three key steps are involved in the pathogenesis of PPIX-mediated phototoxicity in EPP: (i) delivery of PPIX to the skin, (ii) light-triggered PPIX excitation and ROS production, and (iii) ROS-mediated cellular damages<sup>4,6,16</sup>. Theoretically, suppression of each of these three steps will protect against EPP-associated phototoxicity.

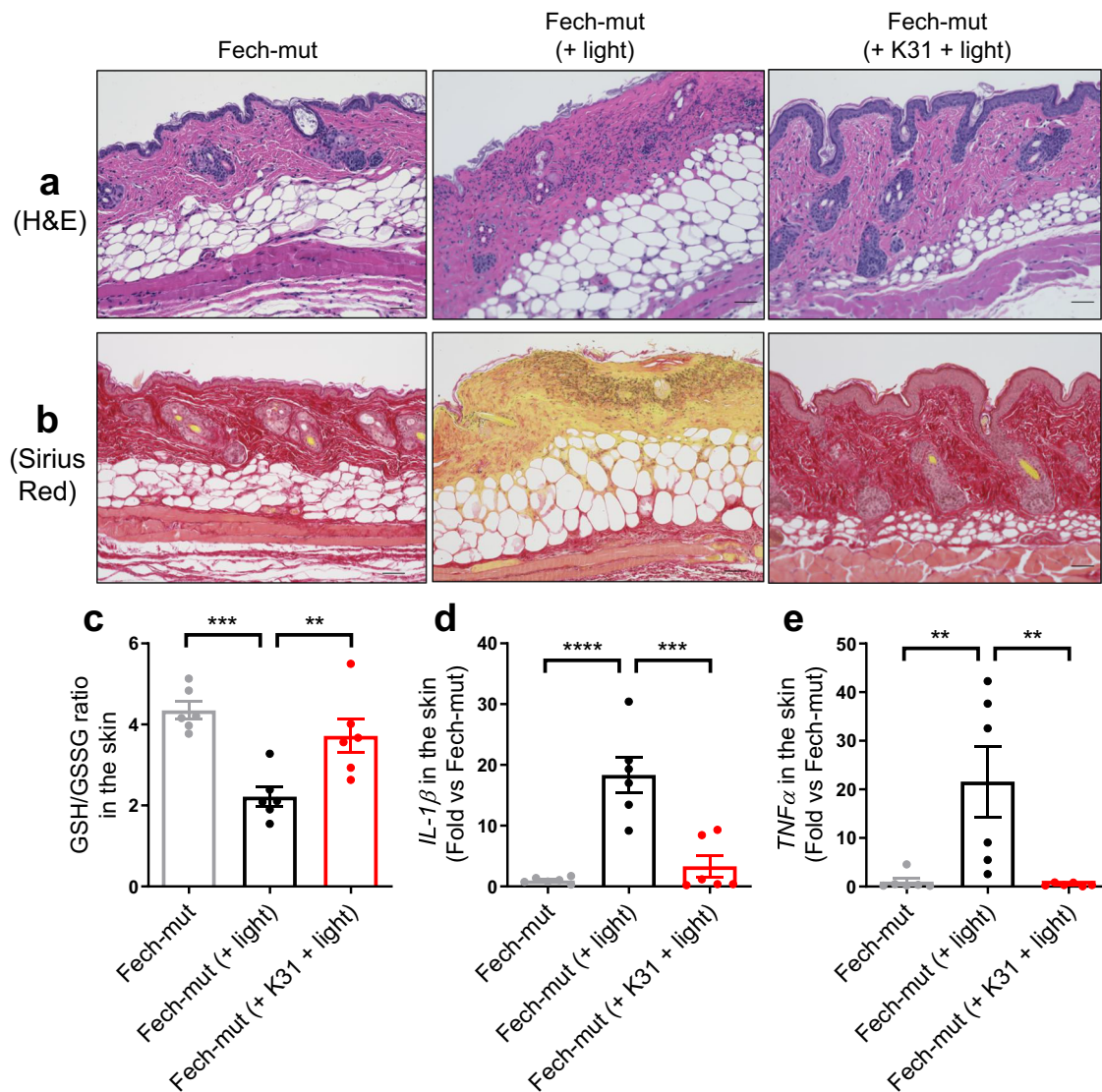


**Fig. 2 | K31 attenuates necrosis, oxidative stress, and inflammation in the skin of an EPP mouse model.** Fech-mut mice (male) were pretreated with K31 (100 mg/kg, po) for 40 min followed by light exposure (once daily for 5 days).

**a, b** Histological analyses of the skin with hematoxylin and eosin (H&E) or Sirius Red staining. Scale bars, 50  $\mu$ m. **c** The ratio of glutathione (GSH) to glutathione disulfide (GSSG) in the skin. GSH and GSSG were analyzed by UPLC-QTOFMS.  $***P = 0.0004$ ,

$**P = 0.0082$ . **d, e** Expression of interleukin 1 $\beta$  (*Il-1 $\beta$* ) and tumor necrosis factor  $\alpha$  (*Tnfa*) in the skin. *Il-1 $\beta$*  and *Tnfa* were analyzed by qPCR. For the date in Fig. 2d,  $****P < 0.0001$ ,  $***P = 0.0002$ ; for the date in Fig. 2e,  $**P = 0.0093$ ,  $**P = 0.0077$ . All data are expressed as mean  $\pm$  SEM ( $n = 6$  mice). One-way ANOVA with Tukey's multiple comparisons tests were used for statistical analysis. Source data are provided as a Source Data file.

Afamelanotide targets step (ii) by increasing skin pigmentation, and in turn decreasing light penetration and reducing light-triggered PPIX excitation and ROS production<sup>9,24</sup>. Antioxidants potentially target step (iii) by quenching ROS and protecting against ROS-mediated cellular damages<sup>12-15</sup>. Our current work provides evidence that ABCG2 inhibitors target step (i) to reduce PPIX transport from erythroid cells to plasma and therefore decrease its delivery to the skin.

Apart from EPP, X-linked protoporphyria (XLP) is another type of porphyria caused by gain-of-function mutations of delta-aminolevulinic acid synthase 2, the rate-limiting enzyme in the heme biosynthesis pathway, leading to PPIX over-production and accumulation<sup>25,26</sup>. XLP shares the same biochemical basis and clinical phenotypes as EPP and also has limited therapeutic options<sup>12,13,25,26</sup>. Based upon the present study on EPP, we expect that ABCG2 inhibitors could also be used for the prevention of PPIX-mediated phototoxicity in XLP.

Our short-term and sub-chronic studies in mice showed that treatment with K31 did not alter growth, the ratios of organ to body weight, and the biomarkers of bone marrow, liver, and kidney toxicity,

suggesting that ABCG2 inhibitors are unlikely to cause adverse effects on these organs. We also do not expect toxicities from ABCG2 suppression itself because: (i) growth and breeding of *Abcg2*-deficient mice are normal, and no health issue was observed in these mice<sup>19</sup>; (ii) compared to Fech-mut mice, the health condition of Fech-mut/*Abcg2*-null mice is significantly better even with a high level of PPIX in RBCs<sup>19</sup>, which is consistent with a previous report showing that the Fech-mut mice in SJL background have a higher level of erythrocyte PPIX but less severe liver damage than the Fech-mut mice in BALB/c and C57BL/6 backgrounds<sup>27</sup>; and (iii) humans with a genetic deficiency of ABCG2 live normally and show no associations with any particular diseases<sup>28-30</sup>. Despite the facts mentioned above, long-term studies are needed to further profile the safety of ABCG2 inhibitors for EPP therapy because EPP is a life-long disease. Further studies are also needed to determine the fate of erythrocyte PPIX under ABCG2 suppression.

In summary, the current work has established a novel strategy against EPP-associated phototoxicity by inhibiting ABCG2. Our work

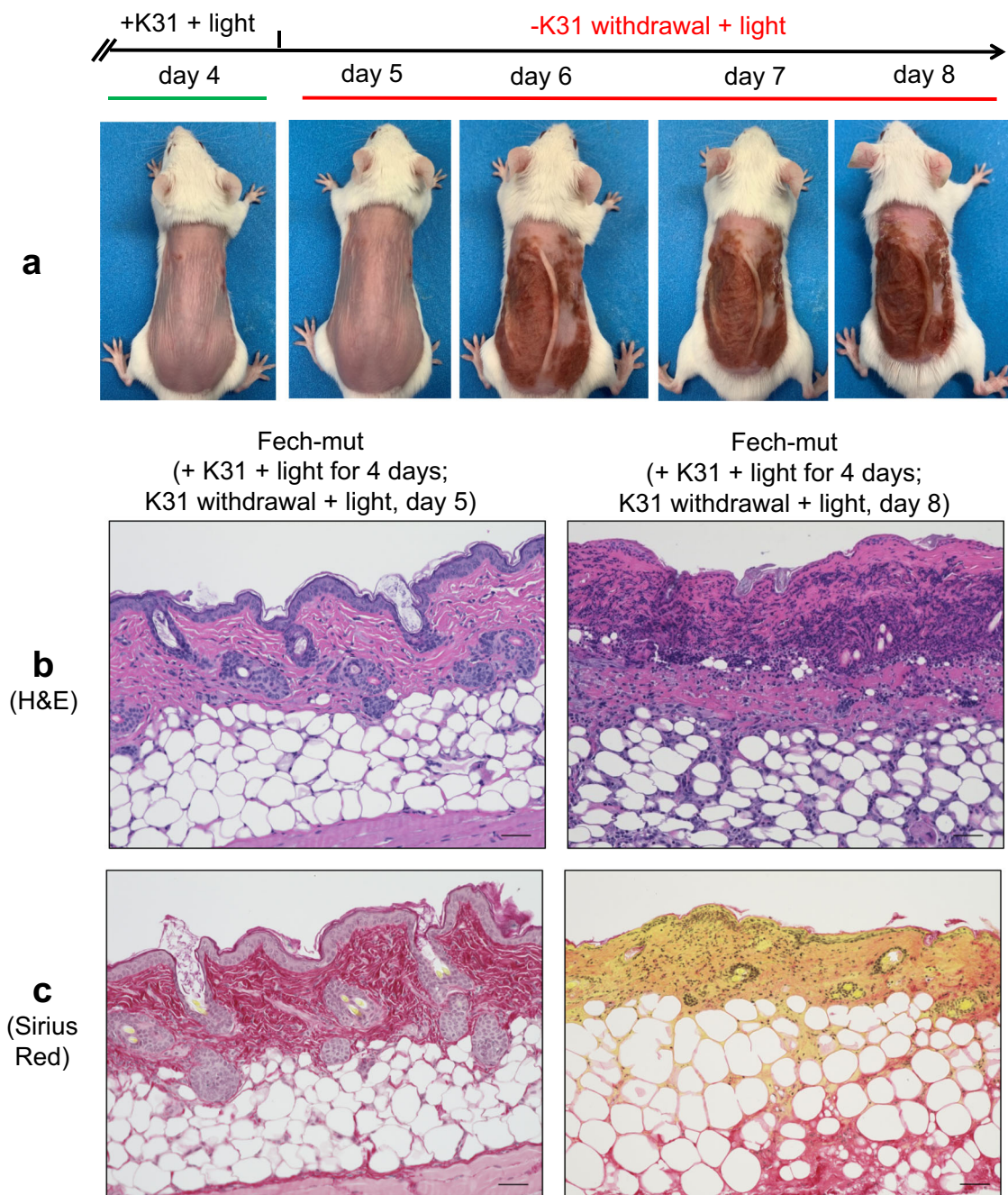


**Fig. 3 | The impact of K31 withdrawal on phototoxicity in Fech-mut mice.** The mice (female,  $n = 3$ ) were pretreated with K31 for 40 min followed by light exposure for 20 min, once daily for 4 days. Afterward, K31 was withdrawn, but the exposure to light (20 min/day) continued for 4 more days. **a** Gross appearance of the skin

after K31 withdrawal. The pictures were taken from the same mouse on different days. **b, c** Histological analyses of the skin with hematoxylin and eosin (H&E) or Sirius Red staining after K31 withdrawal. Scale bars, 50  $\mu\text{m}$ .

could fill a therapeutic gap in EPP by providing oral ABCG2 inhibitors for preventing PPIX-mediated phototoxicity.

## Methods

### Animals and reagents

Fech-mut mice (BALB/c background) were purchased from the Jackson Laboratory (Bar Harbor, ME), and Fech-mut/Abcg2-null mice were developed as recently described<sup>19</sup>. All mice were housed in a temperature and humidity-controlled room (23 °C, 45%) with an alternating 12-h dark and light cycle. CO<sub>2</sub> was used to euthanize mice. The reporting of mouse experiments in this study abides by the ARRIVE guidelines. All protocols for mouse studies in the current work were approved by the Institutional Animal Care and Use Committee of the

University of Pittsburgh. PPIX, 5-aminolevulinic acid (ALA), glutathione (GSH), and glutathione disulfide (GSSG) were purchased from Sigma-Aldrich (St. Louis, MO). Reduced  $\beta$ -nicotinamide adenine dinucleotide phosphate (NADPH) was purchased from Cayman (Ann Arbor, MI). Human liver microsomes (HLM) were purchased from XenoTech (Lenexa, KS). Ko143 was purchased from MedChemExpress (Monmouth Junction, NJ).

### Synthesis of Ko143 analogs

The route for the synthesis of Ko143 analogs is shown in Supplementary Fig. 2. Briefly, compound **1** was synthesized following previous reports<sup>31,32</sup>. Through condensation followed by intramolecular cyclization, *N*-Fmoc-*L*-aspartic acid 4-benzyl ester reacted with compound **1** to

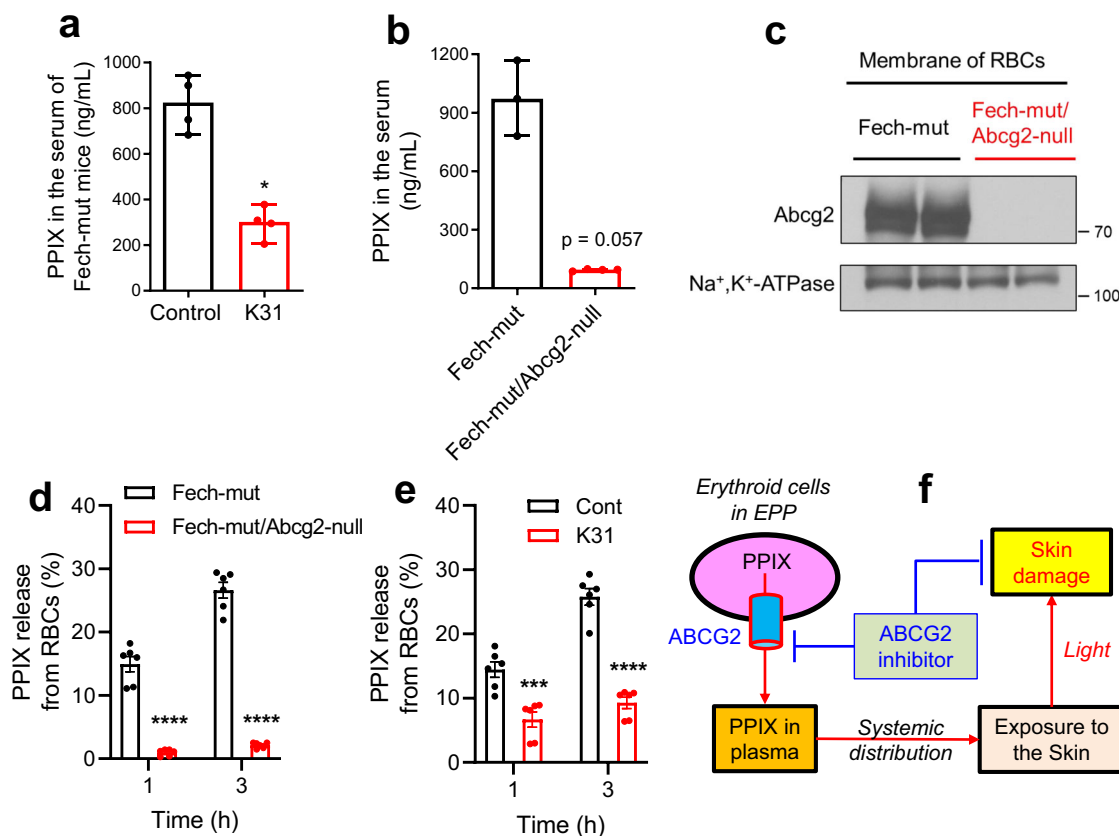


**Fig. 4 | Suppression of ABCG2 modulates PPIX distribution in EPP.**

**a** Quantification of PPIX in the sera of Fech-mut mice treated orally with vehicle (control,  $n = 4$  mice) or K31 (100 mg/kg,  $n = 4$  mice). **b** PPIX levels in the sera of Fech-mut and Fech-mut/Abcg2-null mice ( $n = 3$  mice for Fech-mut group,  $n = 4$  mice for Fech-mut/Abcg2-null group). PPIX in serum was analyzed by UPLC-QTOFMS. Data are expressed as median with range. Two-tailed Mann-Whitney tests were used for statistical analysis,  $*P = 0.0286$ . **c** Expression of Abcg2 in the membrane of red blood cells (RBCs). Na<sup>+</sup>,K<sup>+</sup>-ATPase was used as a loading control for Western blotting. The effect of ABCG2 deficiency (**d**) or

inhibition (**e**) on the percentage of PPIX efflux from RBCs. RBCs were collected from Fech-mut and Fech-mut/Abcg2-null mice and cultured with K31 (10  $\mu$ M) or without K31 (Cont) for 1 or 3 h ( $n = 3$  for each genotype, duplicate incubations for each sample). PPIX in the culture medium of RBCs was analyzed by fluorescence. Data are expressed as mean  $\pm$  SEM.  $***P = 0.0009$ ,  $****P < 0.0001$ , two-tailed  $t$  test. **f** A scheme showing that ABCG2 inhibitors prevent phototoxicity in EPP by modulating PPIX distribution. Source data are provided as a Source Data file.

form **K16**. Deprotection of the benzyl group in **K16** by hydrogenation gave the acid **K17**, which was further coupled with various substituted amines to yield the final Ko143 analogs, including **K3**, **K23**, **K25**, **K31**, and **K33**. The structures of these Ko143 analogs were verified by high resolution mass spectrometry and nuclear magnetic resonance (NMR).

#### ABCG2 inhibitory activity of Ko143 analogs

The A549 cells (ATCC, CCL-185) were seeded onto 12-well plates (300,000 cells per well) and cultured in DMEM medium (Sigma-Aldrich, St. Louis, MO) overnight at 37°C. Next, 1 mM ALA, a precursor of PPIX, was added to the culture medium and incubated for 4 h. Afterward, the culture medium was replaced by fresh medium containing different concentrations of Ko143 or Ko143 analogs. After 2 h incubation, the medium was removed and the cells were washed twice with 1 mL of 1 $\times$  phosphate-buffered saline (PBS, pH 7.4). Then cell lysates were prepared to measure PPIX by ultra-performance liquid chromatography-quadrupole time of flight mass spectrometry (UPLC-QTOFMS, Waters Corporation, Milford, MA).

#### Metabolic stability of Ko143 analogs

Metabolic stability of Ko143 analogs was determined by in vitro studies using HLM and in vivo studies using wild-type (WT, male) mice. Briefly, the in vitro incubations were performed in 1  $\times$  PBS, containing 1 mg/mL HLM, 1 mM NADPH, and 20  $\mu$ M Ko143 or Ko143 analogs in a final volume of 100  $\mu$ L. The reactions were conducted at

37°C for up to 60 min. For in vivo studies, WT mice were treated with 100 mg/kg Ko143 or K31 (po). Blood samples were collected at 0, 0.5, 1, 2, 4, 8, 12, and 24 h after drug treatment ( $n = 4$  at each time point). The concentrations of Ko143 and Ko143 analogs in HLM incubations or mouse sera were analyzed by UPLC-QTOFMS.

#### Cytotoxicity assays

The cytotoxicity of Ko143 analogs was evaluated by the MTT assay. Briefly, A549 cells were seeded onto 96-well plates at a density of 3000 cells/well in DMEM medium. After 16 h incubation, different concentrations of test compounds were added and cells were cultured for 72 h. Afterward, the culture medium was replaced by fresh medium with 0.5 mg/ml MTT and incubated for 3 h. Finally, the supernatant was removed, and cell lysates were prepared and read by spectrophotometer. The half-cytotoxic concentration ( $CC_{50}$ ) of Ko143 analogs was calculated by Graph-Pad Prism 9.

#### Effects of ABCG2 suppression on EPP-associated phototoxicity

The hair on the back skin of Fech-mut mice (both male and female) was removed and the mice were then treated orally with Ko143 or K31 (30 and 100 mg/kg). Forty min later, these mice were exposed to DULEX Flashlight (395–410 nm, 294 lumens (lm)/m<sup>2</sup>) for 20 min. This treatment was repeated once daily for 5 days. For the withdrawal test of K31, Fech-mut mice were pretreated with K31 (100 mg/kg, po) followed by

light exposure (20 min) from the 1<sup>st</sup> to 4<sup>th</sup> day. From the 5<sup>th</sup> to 8<sup>th</sup> day, K31 treatment was stopped, but the exposure to light continued. The gross appearance of mouse skin was recorded every day. All mice were sacrificed 4 h after the last treatment. The back skin, liver, and blood samples were harvested for further analysis.

### Clinical biochemistry

Blood mean corpuscular hemoglobin (MCH) and total hemoglobin (tHb) were analyzed by HESKA HemaTrue (Loveland, CO) and AVOXimeter 4000 (Edison, NJ), respectively. Serum alanine aminotransferase (ALT), aspartate transaminase (AST), and alkaline phosphatase (ALP) were analyzed according to the procedures of standard assay kits from Pointe Scientific Inc (Canton, MI).

### Histological analysis

Skin, liver, and kidney tissues were fixed in 4% formaldehyde phosphate solution overnight and then dehydrated and embedded in paraffin. Four  $\mu\text{m}$  sections were cut for staining. For hematoxylin and eosin (H&E) staining, tissue sections were stained in hematoxylin solution for 5 min, washed with tap water for 1 min, differentiated in 1% acetic acid solution for 1 min, and then stained in eosin solution for 1 min. For Sirius Red staining, tissue sections were stained in 0.1% Picro-Sirius Red solution for 1 h, and then washed twice with 1% acetic acid solution.

### Sub-chronic study of K31

WT mice (male, 8 weeks old) were treated orally with vehicle (control,  $n = 4$ ) or K31 (100 mg/kg,  $n = 4$ ) for 23 days. The body weight of each mouse was measured every day before treatment. On day 24, all mice were sacrificed to collect blood, liver, kidney, and spleen. The ratios of organ to body weight were calculated. In addition, serum biomarkers of liver functions, including ALT, AST, and ALP, were measured by enzymatic assay kits (Point Scientific Inc, Canton, MI). Furthermore, histological analysis was conducted to determine the effect of K31 on the liver.

### Effects of ABCG2 suppression on PPIX distribution in serum

Fech-mut mice (male) were treated with or without K31 (100 mg/kg, po). Thirty min later, the mice were sacrificed to collect blood. Blood samples were also collected from Fech-mut and Fech-mut/Abcg2-null mice (male) without any treatment. To measure PPIX, 20  $\mu\text{L}$  of serum was mixed with 80  $\mu\text{L}$  methanol/acetonitrile (1:1, v/v) and then centrifuged at 21,130 g for 10 min. Two  $\mu\text{L}$  of supernatant was injected into the UPLC-QTOFMS system for PPIX analysis.

### Role of ABCG2 in PPIX efflux from RBCs

To determine the effect of ABCG2 deficiency on PPIX efflux from RBCs, blood samples were collected from Fech-mut and Fech-mut/Abcg2-null mice (female). RBCs were isolated and cultured in RPMI 1640 medium without phenol red (Thermo Fisher Scientific, Waltham, MA), according to previous reports<sup>33,34</sup>. Next, RBCs were seeded onto 48-well plates at a density of  $2 \times 10^8$  cells per well in a final volume of 200  $\mu\text{L}$ . RBCs were incubated at 37 °C with gentle shaking and light protection by aluminum foil. After 1 h and 3 h, the culture medium in each well was collected for PPIX analysis. To determine the effect of ABCG2 inhibitors on PPIX efflux, RBCs from Fech-mut mice were incubated with the culture medium containing K31 (10  $\mu\text{M}$ ) for up to 3 h. Afterward, the culture medium was collected for PPIX analysis by fluorescence detection ( $\lambda_{\text{ex}} = 405 \text{ nm}$ ;  $\lambda_{\text{em}} = 630 \text{ nm}$ )<sup>35</sup>. PPIX levels in RBCs at 0 timepoint of incubation were also measured to determine the percentage of PPIX release from RBCs with ABCG2 deficiency or inhibition.

### Analyses of PPIX and other compounds

The analysis of PPIX was performed on an Acquity UPLC BEH C18 column coupled with a SYNAPT G2-S mass spectrometer (Waters Corporation, Milford, MA). The QTOFMS system was operated in a

positive mode with electrospray ionization. The source and desolvation temperatures were set at 150 and 500 °C, respectively. The capillary and cone voltages were set at 0.8 kV and 40 V. Light protection was considered in the whole process of PPIX analysis. The method for PPIX detection by UPLC-QTOFMS is highly reproducible with an inter-day difference <5% (Supplementary Fig. 10a). In addition, we developed a method for PPIX detection by using a fluorescence plate reader (Biotek, Winooski, VT), which is also reproducible with an inter-day difference <10% (Supplementary Fig. 10b). Furthermore, Ko143, Ko143 analogs, GSH, GSSG, and paclitaxel were also analyzed by UPLC-QTOFMS.

### Statistical analysis

Dependent on groups and sample sizes, statistical analyses were conducted using Mann–Whitney test, Kruskal–Wallis test, one-way or two-way analysis of variance (ANOVA), or two-tailed Student's *t* test. All statistical analysis was performed by GraphPad Prism 9.0. A *P* value < 0.05 was considered statistically significant.

### Reporting summary

Further information on research design is available in the Nature Portfolio Reporting Summary linked to this article.

### Data availability

All data needed to evaluate the conclusions in the paper are present in the main text and the supplementary information. Source data are provided with this paper.

### References

1. Becker, D. M., Viljoen, J. D., Katz, J. & Kramer, S. Reduced Ferrochelatase Activity: a Defect Common to Porphyrria Variegata and Protoporphyrria. *Br. J. Haematol.* **36**, 171–179 (1977).
2. Kramer, S. & Viljoen, J. D. Erythropoietic protoporphyria: evidence that it is due to a variant ferrochelatase. *Int. J. Biochem.* **12**, 925–930 (1980).
3. Scholnick, P., Marver, H. S. & Schmid, R. Erythropoietic protoporphyria: evidence for multiple sites of excess protoporphyrin formation. *J. Clin. Invest.* **50**, 203–207 (1971).
4. Brun, A. & Sandberg, S. Mechanisms of photosensitivity in porphyric patients with special emphasis on erythropoietic protoporphyria. *J. Photochemistry Photobiol. B Biol.* **10**, 285–302 (1991).
5. Rimington, C. Spectral-absorption coefficients of some porphyrins in the Soret-band region. *Biochemical J.* **75**, 620–623 (1960).
6. Cox, G. S., Whitten, D. G. & Giannotti, C. Interaction of porphyrin and metalloporphyrin excited states with molecular oxygen. Energy-transfer versus electron-transfer quenching mechanisms in photo oxidations. *Chem. Phys. Lett.* **67**, 511–515 (1979).
7. Naik, H. et al. Evaluating quality of life tools in North American patients with erythropoietic protoporphyria and X-linked protoporphyria. *JIMD Rep.* **50**, 9–19 (2019).
8. Lecha, M., Puy, H. & Deybach, J. C. Erythropoietic protoporphyria. *Orphanet J. Rare Dis.* **4**, 19 (2009).
9. Langendonk, J. G. et al. Afamelanotide for erythropoietic protoporphyria. *N. Engl. J. Med.* **373**, 48–59 (2015).
10. Wensink, D., Wagenmakers, M. & Langendonk, J. G. Afamelanotide for prevention of phototoxicity in erythropoietic protoporphyria. *Expert Rev. Clin. Pharm.* **14**, 151–160 (2021).
11. Puy, H., Gouya, L. & Deybach, J. C. Porphyrrias. *Lancet* **375**, 924–937 (2010).
12. Balwani, M. Erythropoietic Protoporphyrria and X-Linked Protoporphyrria: pathophysiology, genetics, clinical manifestations, and management. *Mol. Genet. Metabol.* **128**, 298–303 (2019).
13. Minder, E. I., Schneider-Yin, X., Steurer, J. & Bachmann, L. M. A systematic review of treatment options for dermal photosensitivity in erythropoietic protoporphyria. *Cell Mol. Biol.* **55**, 84–97 (2009).

14. Boffa, M., Ead, R., Reed, P. & Weinkove, C. A double-blind, placebo-controlled, crossover trial of oral vitamin C in erythropoietic protoporphyria. *Photodermatol. Photoimmunol. Photomed.* **12**, 27–30 (1996).
15. Mathews-Roth, M., Rosner, B., Benfell, K. & Roberts, J. A double-blind study of cysteine photoprotection in erythropoietic protoporphyria. *Photodermatol. Photoimmunol. Photomed.* **10**, 244–248 (1994).
16. Hussain, Z., Qi, Q., Zhu, J., Anderson, K. E. & Ma, X. Protoporphyrin IX-induced phototoxicity: Mechanisms and therapeutics. *Pharmacol. Ther.* **248**, 108487 (2023).
17. Jonker, J. W. et al. The breast cancer resistance protein protects against a major chlorophyll-derived dietary phototoxin and protoporphyria. *Proc. Natl Acad. Sci. USA* **99**, 15649–15654 (2002).
18. Zhou, S., Zong, Y., Nay, P. A., Nair, G., Stewart, C. F. & Sorrentino, B. P. Increased expression of the Abcg2 transporter during erythroid maturation plays a role in decreasing cellular protoporphyrin IX levels. *Blood* **105**, 2571 (2005).
19. Wang, P. et al. The essential role of the transporter ABCG2 in the pathophysiology of erythropoietic protoporphyria. *Sci. Adv.* **5**, eaaw6127 (2019).
20. Boulechfar, S. et al. Ferrochelatase structural mutant (Fechm1Pas) in the house mouse. *Genomics* **16**, 645–648 (1993).
21. Tutois, S. et al. Erythropoietic protoporphyria in the house mouse. A recessive inherited ferrochelatase deficiency with anemia, photosensitivity, and liver disease. *J. Clin. Investig.* **88**, 1730–1736 (1991).
22. Allen, J. D. et al. Potent and specific inhibition of the breast cancer resistance protein multidrug transporter in vitro and in mouse intestine by a novel analogue of fumitremorgin C. *Mol. Cancer Therapeutics* **1**, 417–425 (2002).
23. Stacy, A. E., Jansson, P. J. & Richardson, D. R. Molecular pharmacology of ABCG2 and its role in chemoresistance. *Mol. Pharmacol.* **84**, 655–669 (2013).
24. Tintle, S., Alikhan, A., Horner, M. E., Hand, J. L. & Davis, D. M. R. Cutaneous porphyrias part II: treatment strategies. *Int. J. Dermatol.* **53**, 3–24 (2014).
25. Balwani, M. et al. Clinical, biochemical, and genetic characterization of north American patients with erythropoietic protoporphyria and X-linked protoporphyria. *JAMA Dermatol.* **153**, 789–796 (2017).
26. Whatley, S. D. et al. C-terminal deletions in the ALAS2 gene lead to gain of function and cause X-linked dominant protoporphyria without anemia or iron overload. *Am. J. Hum. Genet.* **83**, 408–414 (2008).
27. Abitbol, M. et al. A mouse model provides evidence that genetic background modulates anemia and liver injury in erythropoietic protoporphyria. *Am. J. Physiol. Gastrointest. Liver Physiol.* **288**, G1208–G1216 (2005).
28. Niall, H., Parth, K. & Ian, D. K. Polymorphisms of the Multidrug Pump ABCG2: A Systematic Review of Their Effect on Protein Expression, Function, and Drug Pharmacokinetics. *Drug Metab. Disposition* **46**, 1886 (2018).
29. Zhang, W., Sun, S., Zhang, W. & Shi, Z. Polymorphisms of ABCG2 and its impact on clinical relevance. *Biochem. Biophys. Res Commun.* **503**, 408–413 (2018).
30. Zelinski, T., Coghlan, G., Liu, X. Q. & Reid, M. E. ABCG2 null alleles define the Jr(a-) blood group phenotype. *Nat. Genet.* **44**, 131–132 (2012).
31. Li, Y., Hayman, E., Plesescu, M. & Prakash, S. R. Synthesis of potent BCRP inhibitor—Ko143. *Tetrahedron Lett.* **49**, 1480–1483 (2008).
32. Zhu, J. et al. Metabolism-guided development of Ko143 analogs as ABCG2 inhibitors. *Eur. J. Med. Chem.* **259**, 115666 (2023).
33. Trager, W. & Jensen, J. B. Human malaria parasites in continuous culture. *Science* **193**, 673–675 (1976).
34. Tiffert, T. et al. The hydration state of human red blood cells and their susceptibility to invasion by *Plasmodium falciparum*. *Blood* **105**, 4853–4860 (2005).
35. Markwardt, N. A. et al. 405 nm versus 633 nm for protoporphyrin IX excitation in fluorescence-guided stereotactic biopsy of brain tumors. *J. Biophotonics* **9**, 901–912 (2016).

## Acknowledgements

This work was supported by the National Institute of Diabetes and Digestive and Kidney Diseases (R01DK126875, X.M.). We thank Drs. Bethany Flage and Solomon F. Ofori-Acquah for their assistance with hematology analysis.

## Author contributions

X.M. and J.Z. conceived the project and wrote the manuscript. J.Z., F.Q., S.L., R.G., Q.Q., and J.L. performed the experiments. X.M., J.Z., and J.L. contributed to the new reagents, analytic tools, and animal models. J.Z., K.E.A., P.W., and X.M. contributed to scientific discussion and experimental design.

## Competing interests

X.M., J.Z., and J.L. are inventors on a patent (WO2020236901) and hold equity in Portal Therapeutics, Inc. K.E.A. reports receiving consulting fees, advisory board fees and grants to the university from Alnylam Pharmaceuticals, Recordati Rare Diseases, Mitsubishi Tanabe Pharma America, Disc Medicine and Portal Therapeutics. The remaining authors declare no competing interests.

## Additional information

**Supplementary information** The online version contains supplementary material available at <https://doi.org/10.1038/s41467-024-54969-6>.

**Correspondence** and requests for materials should be addressed to Xiaochao Ma.

**Peer review information** *Nature Communications* thanks Jin Wang, and the other, anonymous, reviewer(s) for their contribution to the peer review of this work. A peer review file is available.

**Reprints and permissions information** is available at <http://www.nature.com/reprints>

**Publisher's note** Springer Nature remains neutral with regard to jurisdictional claims in published maps and institutional affiliations.

**Open Access** This article is licensed under a Creative Commons Attribution-NonCommercial-NoDerivatives 4.0 International License, which permits any non-commercial use, sharing, distribution and reproduction in any medium or format, as long as you give appropriate credit to the original author(s) and the source, provide a link to the Creative Commons licence, and indicate if you modified the licensed material. You do not have permission under this licence to share adapted material derived from this article or parts of it. The images or other third party material in this article are included in the article's Creative Commons licence, unless indicated otherwise in a credit line to the material. If material is not included in the article's Creative Commons licence and your intended use is not permitted by statutory regulation or exceeds the permitted use, you will need to obtain permission directly from the copyright holder. To view a copy of this licence, visit <http://creativecommons.org/licenses/by-nc-nd/4.0/>.

© The Author(s) 2024